Journal of Materials Chemistry B

ROYAL SOCIETY OF CHEMISTRY

PAPER

View Article Online
View Journal | View Issue

Check for updates

Cite this: *J. Mater. Chem. B*, 2020, **8**, 10172

Tailoring cellular microenvironments using scaffolds based on magnetically-responsive polymer brushes†

Weronika Górka-Kumik, ‡[ab] Paula Garbacz,‡[bc] Dorota Lachowicz,[d] Paweł Dąbczyński,[a] Szczepan Zapotoczny[b] and Michał Szuwarzyński *[d]

Received 30th July 2020,
Accepted 11th October 2020

DOI: 10.1039/d0tb01853h

rsc.li/materials-b

A variety of polymeric scaffolds with the ability to control cell detachment has been created for cell culture using stimuli-responsive polymers. However, the widely studied and commonly used thermo-responsive polymeric substrates always affect the properties of the cultured cells due to the temperature stimulus. Here, we present a different stimuli-responsive approach based on poly(3-acrylamidopropyl)trimethylammonium chloride) (poly(APTAC)) brushes with homogeneously embedded superparamagnetic iron oxide nanoparticles (SPIONs). Neuroblastoma cell detachment was triggered by an external magnetic field, enabling a non-invasive process of controlled transfer into a new place without additional mechanical scratching and chemical/biochemical compound treatment. Hybrid scaffolds obtained in simultaneous surface-initiated atom transfer radical polymerization (SI-ATRP) were characterized by atomic force microscopy (AFM) working in the magnetic mode, secondary ion mass spectrometry (SIMS), and X-ray photoelectron spectroscopy (XPS) to confirm the magnetic properties and chemical structure. Moreover, neuroblastoma cells were cultured and characterized before and after exposure to a neodymium magnet. Controlled cell transfer triggered by a magnetic field is presented here as well.

Introduction

For the last two decades, large efforts have been made to understand and control the chemical, physical and biological properties of scaffolds for cell cultures.[1,2] A rapid development in the design of materials with interfaces enabling the controlled adsorption and desorption of biological structures is caused by a number of applications requiring the attraction of cells, proteins or DNA layers, followed by their detachment from the surface at the desired moment.[3] However, the precise tailoring of the surface chemistry and physical modifications, while keeping their biocompatible properties for efficient cell culturing, makes those materials difficult in processing. Materials obtained using surface-assembled methods, *e.g.*, multilayer polyelectrolyte films,[4] hydrogels,[5] self-assembled monolayers[6] and polymer brushes[7] are very promising due to their facile preparations and the versatility of the applied compounds. Furthermore, polymer brushes[8,9] provide important interfacial properties for cell culture scaffolds, such as controlled surface swelling and wettability, adjustable macromolecular parameters (molar mass, grafting density, crosslinking ratio), multifunctional character and easy susceptibility for modifications,[10,11] possibility of shape and conformation changes, and full compatibility to most of the support chemistries.[12] Moreover, the polymer brush matrix ensures the surface concentration of the active groups, controlled order of nanoparticles, their adjustable density and ease in modulating the distance of the nanoparticles from the surface.[13] Due to the lack of entanglements, the polymer brushes are characterized by the higher chain flexibility compared to the conventional polymer films that make their stimuli-responsive reaction faster.[14]

The intelligent interfaces, especially stimuli-responsive polymers, are recognized as valuable functional materials in the fields of diagnostics,[15] antibacterial coatings,[16,17] sensing,[16,18]

[a] *Jagiellonian University, Faculty of Physics, Astronomy and Applied Computer Science, Łojasiewicza 11, 30-348 Krakow, Poland*
[b] *Jagiellonian University, Faculty of Chemistry, Gronostajowa 2, 30-387 Krakow, Poland*
[c] *Polish Academy of Sciences, Institute of Organic Chemistry, Kasprzaka 44/52, 01-224 Warsaw, Poland*
[d] *AGH University of Science and Technology, Academic Centre for Materials and Nanotechnology, Mickiewicza 30, 30-059 Krakow, Poland. E-mail: szuwarzy@agh.edu.pl*

† Electronic supplementary information (ESI) available: AFM topography images with corresponding cross-sections of poly(APTAC) and poly(APTAC) + SPIONs brushes, performed in the wet mode, before and after applying neodymium magnet; homogeneous distribution of SPIONs in the poly(APTAC) brushes; neuroblastoma cells cultured on poly(APTAC) + SPIONs brushes without PLL layer on the top; SIMS measurements of poly(APTAC) + SPIONs brushes after applying neodymium magnet and cells detachment. See DOI: 10.1039/d0tb01853h

‡ Both authors contributed equally to this work.

controlled substance/drug release,[19,20] separation of biomolecules,[21] cell culture[22,23] and tissue regeneration.[24,25] The crucial process of cell culture affecting the physiological activity of cells (including migration, orientation or proliferation) is their adhesion to the substrate. Likewise, the non-destructive release of the cells from the substrate is a very important prerequisite for the proper cell reproduction, maintaining suitable cellular genetic characteristics and the possibility of further biological usage.[26] Thus, it is very important to be able to control the properties of the biointerface in cell culture. Stimuli-responsive polymer substrates are capable of chemical and conformational changes upon the application of an external factor.[12,27] The adsorption/desorption of the cells may be induced by changing the surface properties using a trigger, such as light,[28] pH,[29] temperature[30] or exposure to an electric or magnetic field.[15,31] Application of the magnetic field to a magnetic-sensitive interface is advantageous as it is an easily applicable and non-invasive external stimulus that also enables the spatial and temporal control of its action.[31] In the field of cell culturing, it is worth noting that most living systems are not sensitive to a magnetic field. It may also enhance the cell proliferation, rendering this type of surface control potentially non-invasive, especially in the detachment of the cell sheets.[32,33] Nonetheless, intrinsically magnetic responsive polymers are rare and generally present poor efficacy in the magnetic response. Therefore, polymer-based magnetic materials are usually prepared by encapsulation of magnetic nanoparticles, *e.g.*, magnetite (Fe_3O_4) or maghemite (γ-Fe_2O_3).[34] However, it is often challenging to embed the nanoparticles into solid materials.[35]

Currently, spreading interest in smart cell culture led to the fabrication of advanced hybrid inorganic/polymer scaffolds.[36] In this work, we have focused on a magnetically-responsive material based on the nanocomposite of superparamagnetic iron oxide nanoparticles (SPIONs)[37] homogeneously distributed within surface-grafted polyelectrolyte brushes obtained in simultaneous surface-initiated atom transfer radical polymerization (SI-ATRP).[38]

The presented approach leads to the formation of a dynamic magnetic thin layer response to a magnetic field that was successfully used as a scaffold culture neuroblastoma cell, and to test the magnetically-triggered detachment of the living cells. Such studies, especially in tumour microenvironments, are of major importance for improving the effectiveness of cancer treatment and understanding the mechanisms of processes governing changes in differentiation status.[39] The rapid development of research in the field of cell culturing significantly affects the need for more sophisticated surfaces, especially to ensure the non-destructive cell detachment, preserving the cellular integrity and creating opportunities for further study of cell behaviour.

Experimental

Materials

SPIONs. Iron(III) chloride hexahydrate (p.a.) and iron(II) chloride tetrahydrate (p.a.) were purchased from Sigma Aldrich (St. Louis, MO, USA). Ammonium hydroxide (25%, p.a.) was purchased from Chempur (Piekary Slaskie, Poland).

Polymer scaffolds. Polished Prime Silicon Wafers were obtained from Cemat Silicon SA (Warszawa, Poland), (3-aminopropyl) triethoxysilane (APTES, 99%), α-bromoisobutyryl bromide (BIB, 98%), triethylamine (Et3N, ≥99.5%), *N*,*N*,*N*′,*N*″,*N*″-pentamethyldiethylenetriamine (PMDETA, 99%), (3-acrylamidoproplyl)trimethylammonium chloride (APTAC, 75% solution in water), copper(I) bromide (99.999%) were all purchased from Sigma Aldrich (St. Louis, MO, USA). Toluene (p.a.), methanol (p.a.), tetrahydrofuran (p.a,), isopropanol (p.a.), and dichloromethane (HPLC grade, 99.8%) were purchased from Chempur (Piekary Slaskie, Poland). Ammonia solution (25% p.a.) and sulfuric acid (≥95% p.a.) were obtained from POCH S. A. (Gliwice, Poland). Hydrogen peroxide (30% p.a.) was purchased from Stanlab (Lublin, Poland). Poly-L-lysine hydrobromide (PLL, mol wt 30 000–70 000, Quality Level-PREMIUM) was purchased from Sigma Aldrich.

Methods

Dynamic light scattering (DLS) analysis was used to determine sizes and zeta potentials of the nanoparticles (Malvern Nano ZS light-scattering apparatus; measurements at 173° scattering angle, 25 °C). The aqueous dispersion of SPIONs was exposed to a 633 nm laser and the time-dependent autocorrelation function of the photocurrent was acquired every 10 s, with 15 acquisitions for each run. The z-averaged mean diameters, polydispersity and distribution profiles of the sample were gathered using Malvern software. The zeta potential measurements were made using the Laser Doppler Velocimetry technique (LDV).

The size, shape and structure of the nanoparticles were determined using transmission electron microscopy (TEM, Tecnai TF 20 X-TWIN (FEI)). After 5 min sonication, the aqueous dispersion of SPIONs was deposited on a copper grid coated with ultrathin carbon film and air-dried at room temperature. The mean particle diameter was determined as a maximum of the Gaussian curve fitted to the histogram created based on the diameters measured for 100 individual particles.

Atomic force microscope (AFM) images were obtained with a Dimension Icon XR atomic force microscope (Bruker, Santa Barbara, CA, USA) working in the air in the PeakForce Tapping (PFT) mode using standard silicon cantilevers of nominal spring constant of 0.40 N m^{-1}, and in the water in the Tapping Mode using cantilevers of normal spring constant of 0.12 N m^{-1}. Magnetic force microscope (MFM) images were acquired using the same microscope and magnetic Co/Cr-coated silicon cantilevers of nominal spring constant of 2 N m^{-1}. The MFM images were captured in the lift mode at 50 nm lift height for the scaffolds and 100 nm for the bare nanoparticles. A potential (3 V) between the tip and the sample was applied for the measurements of the brushes in order to compensate for their positive charge that could otherwise contribute to the magnetic phase signal. The cantilevers were magnetized with a small magnet before the measurements. The thickness measurements were performed at the edges of the scratched layers.

Secondary ion mass spectrometry (SIMS) experiments were performed on an ION TOF TOFSIMS V (Munster, Germany) instrument, equipped with bismuth manganium liquid metal ion source and C60 ion source. The depth profiles of the samples were obtained in interlaced dual beam mode. A 20 keV C_{60}^{+} ion beam was used to sputter a 600 × 600 μm^2 area and Bi_3^{+} 30 keV ion beam was used to analyse a 200 × 200 μm^2 area concentric to the sputtered surface. For all profiles, the minimal mass resolution at the $^{13}CC_2H_{10}N$ (m/z = 61) was above 6500. Mass calibration was performed with the H, H_2, CH, C_2H_2, C_3H_3, and C_4H_4. Depth calibrations were obtained based on the thickness of the respective sample.

Optical microscopy Nikon Eclipse LV150N has been used to visualize the changes in the adhesion of neuroblastoma cells to magnetic and non-magnetic surfaces.

Synthesis of magnetic nanoparticles (SPIONs)

The syntheses of SPIONs nanoparticles were performed by coprecipitation of 0.1622 g $FeCl_3 \cdot 6H_2O$ and 0.0596 g $FeCl_2 \cdot 4H_2O$ in an aqueous medium (the molar ratio of ions Fe(III) : Fe(II) = 2 : 1, solution pH ≈ 2) according to the method described previously.[40] After deoxygenation by purging with argon, the solution was sonicated for 10 min (1 s pulse per every 5 s) in a thermostatic bath at 20 °C (Sonic-6, Polsonic, 480 W). Subsequently, nanoparticles were precipitated by the dropwise addition of 5 mL of 5 M NH_3(aq), and the suspension of the formed nanoparticles was further sonicated for 30 min. To purify the obtained dispersion, the magnetic chromatography was performed. The iron content in the nanoparticles was determined using a classical spectrophotometric method based on the absorbance measurements of the colour complex of iron(II) ions with phenanthroline, and was calculated to be 0.76 mg Fe mL^{-1}.

Synthesis of hybrid scaffolds (poly(APTAC) + SPIONs)

Silicon wafers were washed before polymerization in a "pir-anha" solution (a mixture of H_2SO_4 and H_2O_2 at a 1 : 3 ratio) for 1 h. Thereafter, the wafers were rinsed thoroughly in distilled water and toluene, dried out in a stream of argon, and put immediately into a solution of amide-silane initiator (APTES) in toluene for 24 h. Afterwards, the wafers were rinsed with a copious amount of toluene and dichloromethane, and finally dried in a stream of argon. Subsequently, the samples were immersed in the solvent mixture (containing 5 mL dichloromethane, 0.05 mL of triethylamine (TEA), and 0.05 mL of 2-isobromobutyryl bromide (BIB)) under an argon atmosphere, and left for 1 h at room temperature (see Scheme 1A). The poly(APTAC) brushes were obtained using the ATRP method. (3-Acrylamidopropyl) trimethylammonium chloride monomer (APTAC; 3 mL, 75% solution in water) was added to a mixture of distilled water (0.375 mL) and isopropanol (1.125 mL) with dissolved CuBr (20 mg) under an argon atmosphere at room temperature. Then, *N*,*N*,*N*′,*N*″,*N*″′ pentamethyldiethylenetriamine (PMDETA; 0.1 mL) was injected into a deoxygenated solution and stirred. The reaction mixture was left for 1 h in an ultrasonic bath. After this time, the substrates were carefully cleaned in water, a mixture of propan-2-ol and water (1 : 1), and methanol in an ultrasonic bath for about 10 min in each solution and dried under an argon stream.

The brushes with embedded magnetic nanoparticles were obtained as described above, but the only difference was the addition of 0.2 mL of the SPIONs dispersion (c = 0.76 mg Fe mL^{-1}) to water in the reaction system at the beginning of the ATRP process, as shown in Scheme 1B. Before injection, the SPIONs dispersion was sonicated for 10 minutes.

Cell culture studies

A murine neuroblastoma cell line was chosen due to its low sensitivity to the changing environmental conditions that enable observation of the exclusive influence of scaffolds on cell behaviour. All cells were maintained in DMEM medium (with L-glutamine, 15 mM HEPES, Sigma-Aldrich) supplemented with 5% fetal bovine serum (FBS) (non-USA origin, sterile-filtered, Sigma-Aldrich), 100 U mL^{-1} penicillin, and 100 μg mL^{-1} streptomycin (HyClone). Murine neuroblastoma cell lines were cultured in a humidified incubator under standard conditions (37 °C, 5% CO_2). The cells were sub-cultured every 2 days until an adequate number of cells was obtained for the study. After reaching approximately 75% of full coverage, the cells were trypsinized, seeded on sterile 24-well plates (TC Plate, Cell +, F, for sensitive adherent cells, Sarstedt) with pure silicon substrates and poly(APTAC) or poly(APTAC) + SPIONs scaffolds in the amount of 7.0 × 10^4 cells per cm^2, and incubated for 24 h. The scaffolds were sterilized and coated with poly-L-lysine (PLL) using a standard procedure (Scheme 1C) prior to transferring the cells onto them. 1 mL of sterile tissue culture grade water was added to 4 mg of poly-L-lysine. The stock solution was 100× diluted with sterile water. The culture surface was aseptically

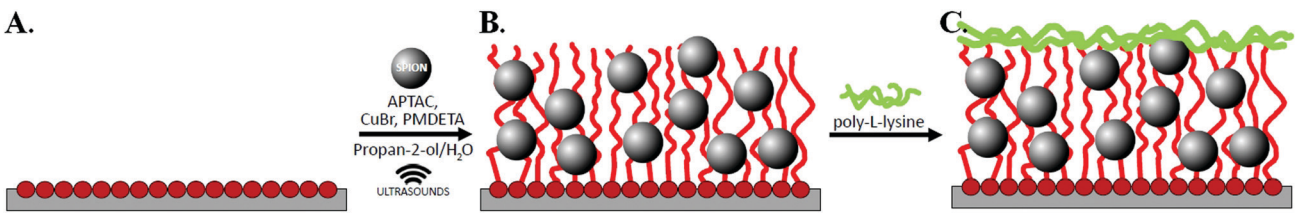

Scheme 1 Schematic drawing of the fabrication of poly(APTAC) + SPIONs scaffolds: (A.) thin layer of surface-grafted initiator (APTES+BIB), (B.) poly(APTAC) brushes obtained in simultaneous ATRP in the presence of SPIONs, (C.) poly(APTAC) brushes with incorporated SPIONs coated with a PLL layer.

coated with 0.5 mL/1 cm^2 (only), and left in an incubator. After 24 h, the solution was removed by aspiration, and the surface was thoroughly rinsed with sterile tissue culture grade water. Subsequently, the cells and medium were introduced into the polymer brush-based scaffolds.

To examine the presence and viability of the cells in the media solution under a magnetic field applied with a neodymium plate magnet (size: 40 × 15 × 5 mm, B = 0.229 T), it was tested during the cell growth using an optical microscope (Carl Zeiss Axio Vert.A1). The neodymium magnets were attached parallel to the substrates with the cultured cells, dipped in medium at a distance of *ca.* 10 mm from the top of the examined surface (one magnet per two wells). The solution was taken from the surface of every scaffold separately after each 24 h and observed microscopically. Viability of neuroblastoma cells on the scaffolds was assessed by the MTT (3-[4,5-dimethylthiazole-2-yl]-2,5-diphenyl tetrazolium bromide) dye conversion assay. Briefly, 7.0×10^4 cells were cultured in 1.1 mL volume of culture medium in a 24-well plate in the presence of different type of scaffolds. Using the MTT test, the viability of the cells cultured on the obtained scaffolds under a magnetic field, as well as their viability in relation to the negative control, such as polystyrene wells, was examined. After 24 h, the cells were washed once and further incubated for 1.5 h with MTT dye. The obtained blue formazan precipitate was dissolved using solubilisation buffer (5 mM HCl in isopropanol), and kept 2 h at 37 °C. The absorbance at 570 nm was then measured using a UV-Vis spectrometer (Thermo Scientific Evolution 220). The results of two independent experiments were averaged, and each of them performed in triplicate. All results were expressed as the means ± standard errors (SEs). The Student's t-test was used to compare data from two groups. A value of $p < 0.05$ was considered significant.

In addition, proliferation tests were performed to examine the influence of the obtained substrates on cells. For this purpose, the Alamar Blue® assay (Invitrogen™, Thermo Fisher Scientific) was used. The test contains a fluorimetric/colorimetric redox indicator that changes from the oxidized (resazurin, non-fluorescent, blue) to reduced form – resorufin (fluorescent, red). The fluorescence/absorbance intensity of resorufin is proportional to the number of living cells, and thus generates a quantitative measurement of cell viability.[41] After 24, 48 and 72 h of culture, the cell viability was studied. The medium was removed and replaced with 10% (vol/vol) AlamarBlue® in DMEM medium, and incubated for 2.5 h at 37 °C (5% CO_2). Subsequently, the medium was transferred from each well in 96-well plates (TC Plate, Cell +, F, for sensitive adherent cells, Sarstedt), and the absorbance was measured at 570 and 600 nm using a microplate reader (TECAN). For further cell culture, they were washed once with PBS buffer and then fresh DMEM medium was added. The proliferation test was performed before and after the magnetic field was applied, as described above.

Results and discussion

Superparamagnetic iron oxide nanoparticles (SPIONs) were successfully embedded into polymer brushes matrix *via* simultaneous surface-initiated atom transfer radical polymerization (SI-ATRP) using the method previously described by us.[38] The SPIONs applied here were obtained by coprecipitation of the individual iron salts in an aqueous medium, and were characterized in terms of their size, stability of their dispersion, and their magnetic properties. The average diameter of the nanoparticles was found to be 8.0 ± 1.1 nm using transmission electron microscopy (Fig. 1A). The surface of the obtained SPIONs was shown to be strongly negatively charged (zeta potential, ξ = −47.6 ± 0.4 mV, Fig. 1B). Thus, their suspension can be considered as stable, which is crucial for the successful running of the polymerization. The magnetic properties were confirmed by magnetic force microscopy (Fig. 1C). All of these parameters correlate well with the previously reported results.[38,40]

The obtained bare polyelectrolyte brushes (poly(APTAC)) and the same brushes with the incorporated SPIONs (poly(APTAC) + SPIONs) were studied using AFM. The thickness of the polymeric layers in the dry state was determined to be 153.2 ± 2.8 nm for the poly(APTAC) brushes and 109.0 ± 2.6 nm for the poly(APTAC) + SPIONs, as shown in Fig. 2A and C, respectively. The smaller thickness of the brushes with the embedded nanoparticles is typical,[38] and it can be briefly explained by the mechanical integration of SPIONs into the polymeric layer by the cross-linking of the chains. The topography images showed distinct differences between both samples. For the poly(APTAC) + SPIONs sample, many objects are sticking out from the underlying smooth polymeric layer. Those objects are not visible in the images of the bare poly(APTAC) brushes. The calculated RMS roughness for a sample with nanoparticles (1.1 ± 0.3 nm) is almost two times bigger than that for the bare poly(APTAC) sample (0.7 ± 0.2 nm). The AFM images indicated the most important aspect of the applied synthesis method, in that there are no aggregates of SPIONs observed on the surface of the poly(APTAC) + SPIONs sample. Both structures were coated with a single layer of PLL, which is known as a good substrate for cell culture.[42] The addition of the polyelectrolyte layer on the top of the brushes caused a significant collapse of the grafted brushes. As shown in Fig. 2B and D, the measured thickness of the dry samples (with the PLL layer on the top) shrunk to the values of 50.4 ± 1.5 nm for the bare poly(APTAC) sample and 38.7 ± 1.2 nm for the poly(APTAC) + SPIONs sample. In the air, the measured RMS roughnesses of both samples only slightly increased to the values of 0.8 ± 0.2 nm

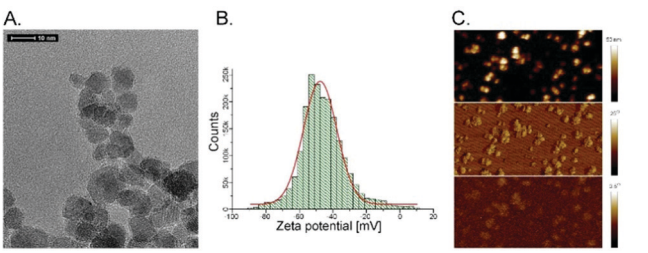

Fig. 1 SPIONs characterization: (A.) HR-TEM image, (B.) histogram of zeta potential values, (C.) AFM-MFM images, scan size = 1 μm (height – top, mechanical phase – middle and magnetic phase – bottom).

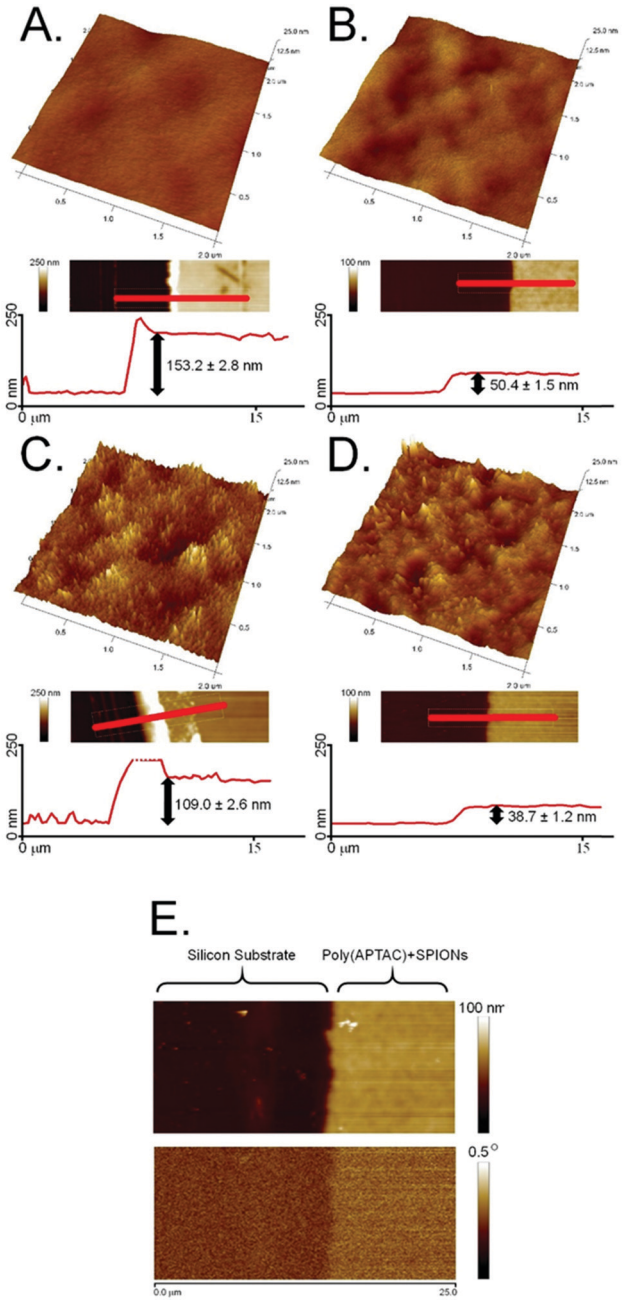

Fig. 2 AFM topography images with corresponding cross-sections of the polymer brushes: (A.) bare poly(APTAC), (B.) poly(APTAC) coated with PLL, (C.) poly(APTAC) + SPIONs brushes and (D.) poly(APTAC) + SPIONs brushes coated with PLL, (E.) MFM phase image of poly(APTAC) + SPIONs brushes coated with PLL (height image – top, magnetic phase – bottom).

for the bare brushes and 1.2 ± 0.4 nm for the brushes with nanoparticles. Due to further biological studies, the obtained scaffolds were investigated in a deionized water environment (pH = 7) before and after neodymium magnet exposition. The RMS roughness of the swollen poly(APTAC) + SPIONs brushes in the water clearly showed a significant change of the surface before (2.8 ± 0.5 nm) and after (4.9 ± 0.9 nm) magnet application. Moreover, no significant difference in the RMS roughnesses was noticed in the reference bare poly(APTAC) brushes: 2.6 ± 0.4 nm before and 2.6 ± 0.5 nm after external magnetic field exposition (see ESI,† Fig. S1). The thickness of the swollen brushes in water was a few times bigger than the thickness in the air: 342 ± 11 nm for poly(APTAC) and 197 ± 8 nm for poly(APTAC) + SPIONs. Furthermore, no significant thickness difference was observed after 24 h in the external magnetic field: 344 ± 10 nm for poly(APTAC) and 195 ± 9 nm for poly(APTAC) + SPIONs (see ESI,† Fig. S2).

The magnetic properties of the scaffold of the poly(APTAC) + SPIONs brushes coated with PLL were confirmed using magnetic force microscopy (MFM). As shown in Fig. 2E, the magnetic signal in the phase image is clearly visible along the whole surface of the hybrid scaffold. In the whole volume of the polymeric layer, a homogeneous distribution of nanoparticles in the poly(APTAC) + SPIONs (with PLL) sample was confirmed using secondary ion mass spectrometry (SIMS). The signal of $^{13}CC_2H_{10}N^+$, which is characteristic of poly(APTAC) brushes, appeared for the measurements of the poly(APTAC) + SPIONs brushes as well. The intensity of the depth profiles (see Fig. 3A and B) stays constant at the beginning during the sputtering process until it decreases when the signal of ^{29}Si for the silicon substrate becomes more intense. Respective isotopes were used to obtain comparable intensities in linear representation. For the poly(APTAC) + SPIONs sample, the signal from the Fe^+ ions for SPIONs is observed in the whole brushes layer. After reaching the silicon substrate, the iron signal does not drop to zero due to the ion beam induced implantation. In the reference sample, a small iron signal is only visible on the silicon substrate surface and it can be considered a silicon contamination. Moreover, the iron and silicon overlay 3D spatial distributions are presented in Fig. 3, respectively, for the poly(APTAC) and poly(APTAC) + SPIONs samples. In the sample with incorporated nanoparticles, it is clearly visible from the iron signal, which comes from SPIONs, that the nanoparticles are homogeneously distributed within the polymer matrix (see ESI,† Fig. S3). Thin iron spots visible in the bare poly(APTAC) sample correspond to the background level (Fig. 3C).

The presence of iron nanoparticles in poly(APTAC) + SPIONs was also confirmed using X-ray photoelectron spectroscopy

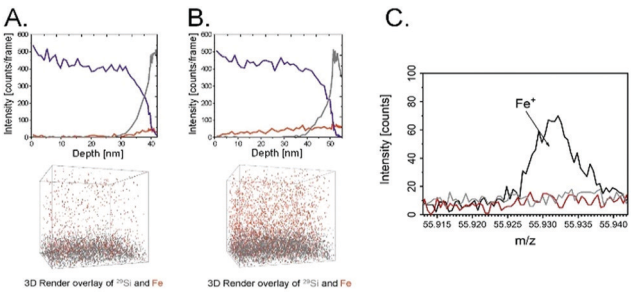

Fig. 3 Secondary ion mass spectrometry (SIMS): depth profiles of poly(APTAC) (A.) and poly(APTAC) + SPIONs coated with PLL (B.) (^{29}Si signal – grey line, $^{13}CC_2H_{10}N$ – violet line, Fe – red line) with corresponding 3D images of spatial distribution of iron (red) and silicon (grey), (C.) fragments of the mass spectra that show the iron signal of the poly(APTAC) + SPIONs brushes (black line), bare poly(APTAC) brushes (red line) and silicon wafer (grey line).

(XPS). As shown in Fig. 4, bands appeared in the spectrum with characteristic binding energies – C1s (284–286 eV), N1s (399–403 eV), O1s (531–533 eV) for the polymer brushes material. Two bands Cl2s (270 eV) and Cl2p (200 eV) existing in the spectrum come from the chlorine present as a counter-ion for the positively charged poly(APTAC) brushes. Moreover, the characteristic band at 709 eV related to $Fe2p_{3/2}$ from SPIONs is visible in the spectrum. XPS data were used to estimate the total amount of iron from SPIONs and other elements from brushes: $Fe2p_{3/2}$ – 0.6%, C1s – 74.6%, N1s – 11.8%, O1s – 11.9%. The obtained results correlate with the previously obtained data for the thin polymer layers with the SPIONs.[38] The N1s band is separated into two peaks: 399 eV for the terminal cationic group $-N^{+}(CH_3)_3$ and 403 eV for –C–N– in the main APTAC chain. Furthermore, the XPS spectra enable the observation of the presence of a thin layer of PLL on the top of the poly(APTAC) + SPIONs brushes. Both bands for N1s are slightly increased and shifted due to the additional –NH– and $-NH_2$ groups from PLL (bright lines in Fig. 4B).[43]

Considering the possible application of the obtained substrates in the cell culture, it is essential to determine the morphology of the cells adhering to the surface of the samples. Before applying the neodymium magnet, all surfaces were studied in terms of the morphology of the cells adhering to the surface of the samples. Therefore, the morphology of the neuroblastoma cells cultured on the poly(APTAC) and poly(APTAC) + SPIONs layers was assessed by means of direct microscopic observations of the uncontrolled cell detachment with no external stimulus. As shown in Fig. 5A, cells adhered well to all presented surfaces. Microscopic images of neuroblastoma cells after 48 h under the applied magnetic field on the polystyrene (control) and the PLL layer on the reference silicon substrate, bare poly(APTAC) brushes, and poly(APTAC) + SPIONs brushes are presented in Fig. 5B. Neuroblastoma cells cultured on poly(APTAC) after applying the magnetic field adhere well to the surface, and exhibit an ordinary morphology comparable to that of the control on the polystyrene and silicon surface (Fig. 5B.1. and B.2.). It can also be observed that the cells are relatively evenly distributed on the surface of the sample. After 48 h under the applied magnetic field, there was no significant difference in the morphology and adhesion of the cells cultured on the bare poly(APTAC) brushes, reference polystyrene or silicon sample (Fig. 5B.3.). In contrast, neuroblastoma cells cultured on the poly(APTAC) + SPIONs brushes are almost completely removed from the surface (Fig. 5B.4.). Some of them remained on the surface, exhibiting shrunken and collapsed morphology. To study the viability of the cells detached from the surfaces, optical microscopy images of the culture medium in multiwell plates were taken. As can be seen, the layers of the cells detach only from the surface of poly(APTAC) + SPIONs under the influence of a magnetic field, and they are visible in the collected medium solution (Fig. 5C.4.). This effect was not observed for the surface of the bare polymer brushes, the reference polystyrene, or the silicon sample (Fig. 5C.1.–C.3.). It is important to note that the detached layers of the cells were found to be alive and in very good condition after the separation, which was confirmed during the optical observation and proliferation tests of the medium solution collected from the surface of the reference polystyrene plate, a control silicon substrate, bare poly(APTAC) brushes and poly(APTAC) + SPIONs brushes. Before optical imaging, the multiwell plate was incubated for 2 h in 37 °C to allow cells to adhere to the new sterile well.

The viability of murine neuroblastoma cells cultured on the poly(APTAC) and poly(APTAC) + SPIONs brushes was determined using the MTT tests. MTT experiments confirmed that the synthesized poly(APTAC) and poly(APTAC) + SPIONs scaffolds allow for appropriate cell growth, and do not cause cytotoxicity. The difference in the cell viability between the control sample (cells cultured directly on a multi-well plate) and cells grown on the surface of the silicon wafers with a poly(APTAC) and poly(APTAC) + SPIONs layer was found to be statistically non-significant. A statistically substantial difference was observed only for cells cultured on a bare silicon substrate (Fig. 6A). Furthermore, the cells cultured on the poly(APTAC) + SPIONs brushes were successfully detached from the surface using the conformational changes of the brushes upon the application of an external magnetic field. The MTT tests showed that less than 50% of the cultured cells remained on the surface of poly(APTAC) + SPIONs compared to the bare poly(APTAC) brushes after using a magnetic field (Fig. 6B). Likewise, the results obtained by proliferation test before applying the magnet (Fig. 6C) showed that neuroblastoma cells seeded onto the four types of scaffolds (polystyrene, silicon, poly(APTAC), poly(APTAC) + SPIONs) were similarly proliferative over time in culture, but the cells seeded onto silicon scaffolds were more proliferative than those seeded onto polystyrene, poly(APTAC) or poly(APTAC) + SPIONs scaffolds. Moreover, the results obtained for the medium collected from the surfaces of each substrate mentioned above after using the magnetic field (Fig. 6D) showed a noticeable difference in the proliferation and amount of cells detached from the poly(APTAC) + SPIONs in respect to the medium collected from the reference polystyrene, silicon substrate or poly(APTAC) brushes. As can be seen, the neuroblastoma cells collected in the medium from the surface of poly(APTAC) + SPIONs were more proliferative after 48 h under an applied magnetic field

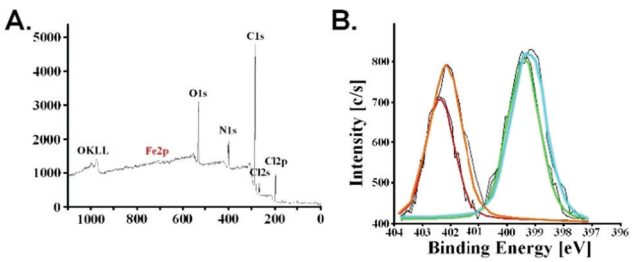

Fig. 4 (A.) X-ray photoelectron spectroscopy (XPS) spectrum of poly(APTAC) + SPIONs and (B.) fragments of the spectra corresponding to the N1s signal of poly(APTAC) + SPIONs with PLL coating (–C(NH)C– – orange line, $-N^{+}(CH_3)_3$ – blue line) and without the coating (–C(NH)C– – red line, $-N^{+}(CH_3)_3$ – green line).

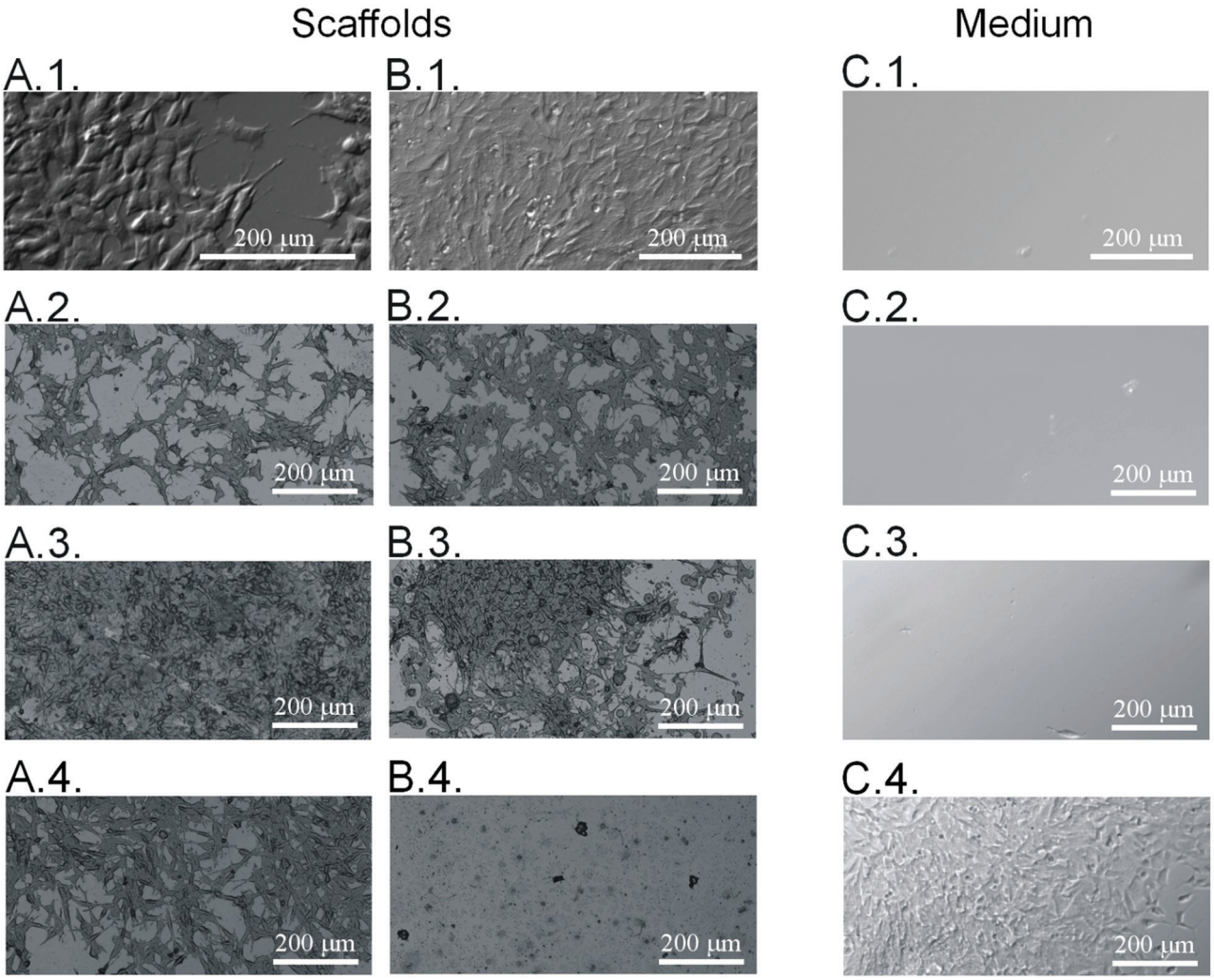

Fig. 5 Optical microscopy images of neuroblastoma cells cultured before (A.) and after (B.) applying an external magnetic field, and the detached cells collected from the medium during application of the magnetic field (C.) of: (1.) Polystyrene, (2.) Silicon modified with PLL, (3.) Poly(APTAC) brushes with PLL, (4.) poly(APTAC) + SPIONs brushes with PLL.

than in medium collected from other substrates. It may be a result of the higher number of cells detached from the surface of poly(APTAC) + SPIONs brushes and collected in the medium. Moreover, neuroblastoma cells detached from the poly(APTAC) + SPIONs substrate using a magnetic trigger present high proliferation, which indicates that the cells exhibit good viability and are in good condition after the separation.

The presented results show that the obtained substrate composed of poly(APTAC) brushes and embedded magnetic nanoparticles supports cell growth. In addition, under the influence of a neodymium magnet, the poly(APTAC) + SPIONs brush layer effectively induces cell detachment.[44] From the AFM topography measurements in the water of the swollen polymer substrates (see ESI,† Fig. S1), it seems that the process of cell detachment from the surface is associated with the conformational changes of the poly(APTAC) brushes with embedded SPIONs, increasing the RMS roughness. This may be due to the displacement of the magnetic nanoparticles towards a neodymium magnet, which was applied at a short distance above the surface of the substrate. As a result, the poly(APTAC) chains are exposed from under the poly-L-lysine layer. The strong cationic properties of the poly(APTAC) chains significantly hinder the neuroblastoma cell culture and proliferation, which is clearly visible in the poly(APTAC) + SPIONs brushes without the PLL layer on the top (see ESI,† Fig. S4). Therefore, the contact of the cells with poly(APTAC) chains causes their detachment from the surface of poly(APTAC) + SPIONs. The use of a magnetic trigger has many advantages and possibilities, and it does not lead to a release of SPIONs from the polymer at the applied conditions. As the SIMS spectra show (see ESI,† Fig. S5) after 48 h in the magnetic field and cell detachment, the SPIONs are still incorporated in the poly(APTAC) brushes. In particular, it is non-invasive when compared to the conventional methods of detaching cell (sheets) from substrates, such as mechanical cell scraping or enzymatic cell uptake, which can be very severe for the obtained cells.[45] On the other hand, due to the temperature stimulus, the widely studied thermo-responsive polymer substrates always

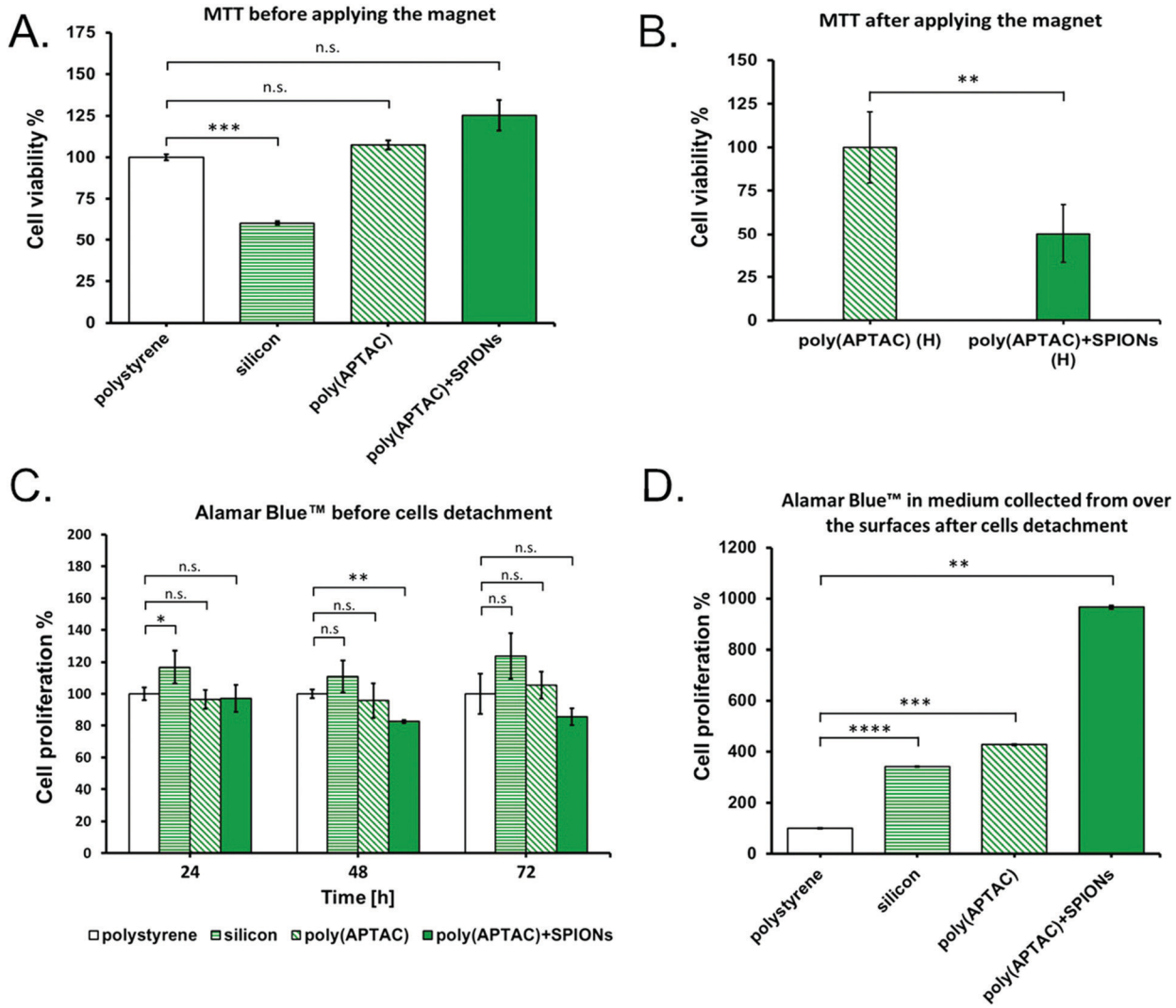

Fig. 6 (A.) Cell viabilities results (MTT assay) for murine neuroblastoma cell lines for reference polystyrene and silicon sample, poly(APTAC) and poly(APTAC) + SPIONs substrate before applying the magnetic field; (B.) MTT assay for neuroblastoma cell lines illustrating the amount of cells remaining on the surface of the poly(APTAC) brushes and poly(APTAC) + SPIONs brushes after exposure to magnetic field (H); (C.) Cell proliferation results determined by Alamar Blue™ assay before cells detachment induced by magnetic field and D. after applying the magnetic trigger and collecting medium with the cells from the surface of substrates. Data are reported as the percentage growth compared to polystyrene (100%). The p values are reported in respect to polystyrene (*$p < 0.05$, **$p < 0.01$, ***$p < 0.001$, ****$p < 0.0001$). Statistical significance was determined by student t test ($n = 3$).

affect the entire cell culture. Therefore, controlling the cell behaviours in localized areas or individual cells cannot be achieved.[46] It should be noted that the detached cells are in good condition and are capable of further growth, which shows great potential for use in tissue engineering. Considering all results presented before, the proposed hybrid polymer–inorganic system of poly(APTAC) + SPIONs brushes seems to be promising as a magnetically responsive substrate for cell culture and controlled harvesting.

Conclusions

In this report, we present a promising material for stimuli-responsive cell culture substrates. The obtained poly(APTAC) + SPIONs brushes were synthesized using an efficient and facile method of incorporation of magnetic nanoparticles (SPIONs) into the cationic polymer brush layer poly(APTAC) *via* surface-initiated ATRP assisted by ultrasounds. The obtained samples were characterized structurally, magnetically and biologically. It is important to note that based on the AFM images, there are no aggregates of SPIONs on the surface of the sample. A magnetic signal from the entire surface of the hybrid scaffold poly(APTAC) + SPIONs brushes was determined by magnetic force microscopy. The homogeneous incorporation of SPIONs into the brushes was also confirmed using 3D images of the spatial distribution of iron and silicon using SIMS and XPS techniques. Moreover, the XPS spectroscopy was used to estimate the total amount of iron from SPIONs in the hybrid scaffold to be 0.6% of the total mass. The neuroblastoma cells cultured on bare poly(APTAC) and poly(APTAC) + SPIONs adhered well to the surface, and exhibited ordinary

morphology. However, after 48 h under the applied magnetic field, only the cells cultured on poly(APTAC) + SPIONs were detached and significantly decreased their amount adhering to the surface. Cell detachment triggered by an external magnetic field enabled the non-invasive and controlled transfer of cultured neuroblastoma cells into a new place without the addition of extra chemical/biochemical compounds. Moreover, the presence of SPIONs in the polymer scaffold and the application of a magnetic field are necessary conditions for the controlled cell transfer. The evident difference between the bare poly(APTAC) brushes and poly(APTAC) + SPIONs brushes seems to indicate that the obtained magnetic-responsive poly(APTAC) + SPIONs hybrid material seems to be a promising controllable scaffold for cell culture. It is also worth noting that all obtained scaffolds, despite differences in the surface roughness and polymer thickness, are not able to detach the cultured cells without the application of a magnetic stimulus.

Conflicts of interest

The authors declare no competing financial interest.

Acknowledgements

W. G.-K., P. G. S. Z. and M. S. would like to thank the Foundation for Polish Science for financial support ((grant number: TEAM/2016-1/9)) and D. L. to National Science Centre (grant number: 2014/15/D/ST4/02770). The research was performed with equipment purchased thanks to the financial support of the European Regional Development Fund in the framework of the Polish Innovation Economy Operational Program (contract no. POIG.02.01.00-12-023/08). Moreover, Marta Gajewska (Academic Centre for Materials and Nanotechnology, AGH) is acknowledged for TEM measurements and Magdalena Wytrwał – Sarna (Academic Centre for Materials and Nanotechnology, AGH) is thanked for an inspiring discussion.

References

1 S. R. Caliari and J. A. Burdick, *Nat. Methods*, 2016, **13**, 405–414.
2 N. Bhardwaj, D. Devi and B. B. Mandal, *Macromol. Biosci.*, 2015, **15**, 153–182.
3 M. A. Cole, N. H. Voelcker, H. Thissen and H. J. Griesser, *Biomaterials*, 2009, **30**, 1827–1850.
4 A. Mikulska, J. Filipowska, A. M. Osyczka, M. Szuwarzyński, M. Nowakowska and K. Szczubiałka, *Cell Prolif.*, 2014, **47**, 516–526.
5 S. Fiejdasz, W. Horak, J. Lewandowska-Łańcucka, M. Szuwarzyński, J. Salwiński and M. Nowakowska, *J. Colloid Interface Sci.*, 2018, **524**, 102–113.
6 P. Y. Wang, H. Pingle, P. Koegler, H. Thissen and P. Kingshott, *J. Mater. Chem. B*, 2015, **3**, 2545–2552.
7 L. Moroni, M. Klein Gunnewiek and E. M. Benetti, *Acta Biomater.*, 2014, **10**, 2367–2378.
8 J. O. Zoppe, N. C. Ataman, P. Mocny, J. Wang, J. Moraes and J. H.-A. Klok, *Chem. Rev.*, 2017, **117**, 1105–1318.
9 K. Wolski, M. Szuwarzyński, M. Kopeć and S. Zapotoczny, *Eur. Polym. J.*, 2015, **65**, 155–170.
10 E. S. Fioretta, J. O. Fledderus, E. A. Burakowska-Meise, F. P. T. Baaijens, M. C. Verhaar and C. V. C. Bouten, *Macromol. Biosci.*, 2012, **12**, 577–590.
11 M. Krishnamoorthy, S. Hakobyan, M. Ramstedt and J. E. Gautrot, *Chem. Soc. Rev.*, 2016, **45**, 377–411.
12 R. H. Kollarigowda, C. Fedele, C. Rianna, A. Calabuig, A. C. Manikas, V. Pagliarulo, P. Ferraro, S. Cavalli and P. A. Netti, *Polym. Chem.*, 2017, **8**, 3271–3278.
13 M. Navarro, E. M. Benetti, S. Zapotoczny, J. A. Planell and G. J. Vancso, *Langmuir*, 2008, **24**(19), 10996–11002.
14 X. Fu, L. Hosta-Rigau, R. Chandrawati and J. Cui, *Chem*, 2018, **4**, 2084–2107.
15 H. Takahashi, T. Shimizu and T. Okano, *Princeton Regenerative Medicine*, Elsevier Inc., 2019, pp. 469–484.
16 J. N. Anker, W. P. Hall, O. Lyandres, N. C. Shah, J. Zhao and R. P. Van Duyne, *Nat. Mater.*, 2008, **7**, 442–453.
17 T. Wei, Q. Yu and H. Chen, *Adv. Healthcare Mater.*, 2019, **8**(1801381), 1–24.
18 T.-U.-H. Shah, M. H. Tahir, M. S. Ahmad, A. Rahman, M. Arshadkamran and H. Liu, *Eur. Polym. J.*, 2020, **124**(109486), 1–7.
19 M. Szuwarzyński, L. Zaraska, G. D. Sulka and S. Zapotoczny, *Chem. Mater.*, 2013, **25**, 514–520.
20 H. Xiong, Y. Wu, Z. Jiang, J. Zhou, M. Yang and J. Yao, *J. Colloid Interface Sci.*, 2019, **536**, 135–148.
21 A. Mizutani, A. Kikuchi, M. Yamato, H. Kanazawa and T. Okano, *Biomaterials*, 2008, **29**, 2073–2081.
22 M. Krishnamoorthy, S. Hakobyan, M. Ramstedt and J. E. Gautrot, *Chem. Rev.*, 2014, **114**, 10976–11026.
23 X. Xue, L. Thiagarajan, S. Braim, B. R. Saunders, K. M. Shakesheff and C. Alexander, *J. Mater. Chem. B*, 2017, **5**, 4926–4933.
24 M. Mirbagheri, V. Adibnia, B. R. Hughes, S. D. Waldman and D. K. Hwang, *Mater. Horiz.*, 2019, **6**, 45–71.
25 S. Zapotoczny, *Nanotechnol. Regener. Med. Methods Proto*, 2012, **811**, 51–78.
26 J. Li, X. Fan, L. Yang, F. Wang, J. Zhang and Z. Wang, *Int. J. Polym. Mater. Polym. Biomater.*, 2018, **67**, 371–382.
27 L. Chunliang and M. W. Urban, *Prog. Polym. Sci.*, 2018, **78**, 24–46.
28 C. Fedele, P. A. Netti and S. Cavalli, *Biomater. Sci.*, 2018, **6**, 990–995.
29 G. Kocak, C. Tuncer and V. Bütün, *Polym. Chem.*, 2017, **8**, 144–176.
30 Y.-J. Kim and Y.-T. Matsunaga, *J. Mater. Chem. B*, 2017, **5**, 4307–4321.
31 J. Thévenot, H. Oliveira, O. Sandre and S. Lecommandoux, *Chem. Soc. Rev.*, 2013, **42**, 7099–7116.
32 S. Kondaveeti, A. Teresa, S. Semeano, D. R. Cornejo, H. Ulrich, D. Freitas and S. Petri, *Colloids Surf., B*, 2018, **167**, 415–424.
33 T. Glaser, V. B. Bueno, D. R. Cornejo, D. F. S. Petri and H. Ulrich, *Biomed. Mater.*, 2015, **10**(045002), 1–11.

34 K. M. Rao, A. Kumar and S. S. Han, *J. Mater. Sci. Technol.*, 2017, **34**, 1371–1377.
35 M. Kohri, K. Yanagimoto, K. Kohaku, S. Shiomoto, M. Kobayashi, A. Imai, F. Shiba, T. Taniguchi and K. Kishikawa, *Macromolecules*, 2018, **51**, 6740–6745.
36 L. Cao, X. Wu, Q. Wang and J. Wang, *J. Photochem. Photobiol., B*, 2018, **178**, 440–446.
37 B. T. Mai, S. Fernandes, P. B. Balakrishnan and T. Pellegrino, *Acc. Chem. Res.*, 2018, **51**, 999–1013.
38 W. Górka, T. Kuciel, P. Nalepa, D. Lachowicz, S. Zapotoczny and M. Szuwarzyński, *Nanomaterials*, 2019, **9**(456), 1–11.
39 A. Edsjö, L. Holmquist and S. Påhlman, *Semin. Cancer Biol.*, 2007, **17**, 248–256.
40 G. Kania, U. Kwolek, K. Nakai, S. I. Yusa, J. Bednar, T. Wójcik, S. Chłopicki, T. Skórka, M. Szuwarzyński, K. Szczubiałka, M. Kępczyński and M. Nowakowska, *J. Mater. Chem. B*, 2015, **3**, 5523–5531.
41 J. Filipowska, J. Lewandowska-Łańcucka, A. Gilarska, Ł. Niedźwiedzki and M. Nowakowska, *Int. J. Biol. Macromol.*, 2018, **113**, 692–700.
42 C. A. Hong, H. Y. Son and Y. S. Nam, *Sci. Rep.*, 2018, **8**, 1–7.
43 S. K. Tam, J. Dusseault, S. Polizu, M. Ménard, J.-P. Halle and L. Yahia, *Biomaterials*, 2005, **6**, 6950–6961.
44 K. Nagase and T. Okano, Thermoresponsive Polymer Brushes for Thermally Modulated Cell Adhesion and Detachment, *Polymer and Biopolymer Brushes: for Materials Science and Biotechnology*, Wiley, 2017.
45 M. E. Nash, D. Healy, W. M. Carroll, C. Elvira and Y. A. Rochev, *J. Mater. Chem.*, 2012, **22**, 19376–19389.
46 L. Chen, C. Yan and Z. Zheng, *Mater. Today*, 2018, **21**, 38–59.